管道电弧声发射特征采集系统设计

刘立君[1,2]，　兰　虎[1]，　段宏伟[1]，　温建力[1]
（1. 哈尔滨理工大学 材料科学与工程学院，哈尔滨　150080；2. 浙江大学 宁波理工学院，浙江 宁波　315100）

摘　要：鉴于焊接电弧声信号中蕴涵着丰富的焊接状态信息，是焊接质量监控重要的源信号，而管道结构特征为电弧声发射信号在管内低噪声传播创造了条件。设计了管道电弧声发射采集硬件系统，主要由传感器、信号适配电路、数据采集卡和一体化工作站组成。采用图形化虚拟仪器编程语言 LabVIEW，通过封装功能模块及调用硬件驱动的动态链接程序，设计了一套采用中断触发方式进行高速数据采集的电弧声发射软件系统。结果表明，该系统不仅能实现对电弧电压、焊接电流和电弧声发射信号的高速实时同步采集，并可将采集结果图形化显示，很好地解决了实时图形绘制难的问题，为进一步研究管道 TIG 焊接电弧声发射机理创造条件。

关键词：管道焊接；电弧声发射；图形化虚拟仪器编程语言
中图分类号：TP274　　文献标识码：A　　文章编号：0253－360X(2008)12－0037－04

刘立君

0　序　　言

近年来，随着管道全位置自动焊接机在国内管道工程上应用，管道打底焊单面焊双面成形成为限制管道全位置自动焊机广泛应用瓶颈技术之一[1,2]。以往基于电弧声特征的焊接熔透控制主要集中在等离子焊接和激光焊接，利用其小孔效应产生电弧声突变特征作为判据[3]。而工程上管道自动化打底焊主要采用非熔化极气体保护焊(TIG)，由于管道焊接结构特点，使得利用各种半导体光敏元件从焊缝背面检测熔池尺寸，间接获取焊缝熔透传感控制方式受到限制[4]。在实际生产中，熟练焊工往往能根据电弧声辨别熔滴过渡方式、焊接过程稳定性、飞溅大小和熔透情况，这说明电弧声可作为焊接质量监测的潜在信息源之一，而管道结构特征为电弧声发射信号在管内低噪声传播创造了条件[5－8]。因此提出建立管道 TIG 焊电弧声发射信号采集硬件系统，在此基础上，借助图形化虚拟仪器编程语言 LabVIEW，设计一套高速实时同步采集存盘软件系统，以实现对电弧电压、焊接电流和电弧声发射信号的拾取，为进一步研究管道 TIG 焊电弧声发射机理以及基于电弧声发射信号特征的管道熔透控制奠定基础。

收稿日期：2007－12－03
基金项目：黑龙江省自然科学基金项目(E2007－01)；宁波自然科学基金重点项目(2008A610031)；黑龙江省青年骨干教师支持项目(1153G009)；哈尔滨市科技创新人才基金项目(2007RFQXG055)

1　管道 TIG 焊接系统

图 1 为全位置 TIG 焊控制系统工作原理图，该焊接操作机具有焊枪行走、焊缝对中及跟踪、钨极摆动、左右送丝、弧长调节等主要控制功能，以及手控盒和辅助控制功能。

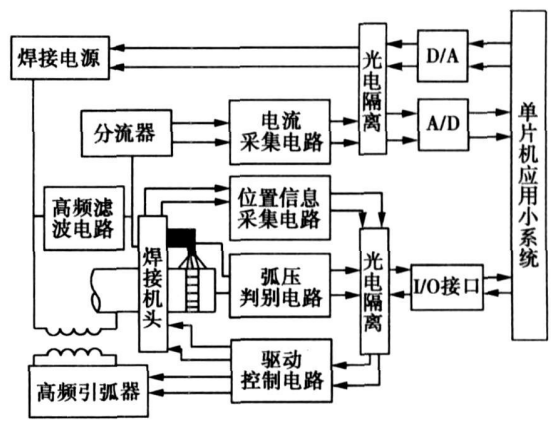

图 1　管道全位置焊控制系统工作原理图

Fig. 1　Schematic of all position pipe-welding control system

在管道全位置焊接中，由于所焊的管材不同，壁厚不同，焊接中电弧运动的实际位置不断变化，要求焊接工艺参数也能够相应地发生变化和调整，行之

有效的方法是适当划分环缝的空间位置。例如，通常将整条环缝划分为 8 个区段，每段的焊接电流、电弧电压、焊接速度和送丝速度等可根据此区段的位置分别给予不同的数值。但在管道的全位置焊接过程中的各个运动部位，如行走(焊接速度)、焊枪摆动、电弧电压的调节等要求与弧焊电源同步，且控制准确度要求较高。

2 采集系统硬件设计

2.1 系统组成原理

在全位置 TIG 焊控制系统基础上建立管道焊接电弧声发射采集系统见图 2，主要由传感器、信号适配电路、采集模块、一体化工作站以及焊接电源等部分组成。系统工作原理是采用两个传声器拾取焊接电弧声发射信号，管外传声器用于监测电弧飞溅、干伸长、弧长、熔透和焊接位置等方面的电弧声发射信号特征；管内传声器主要监测熔透电弧声发射特征。传声器拾取的电弧声、电流传感器采集的焊接电流和电压传感器拾取的电弧电压同步送入信号适配电路，随后 4 路调理信号由终端板 PCLD-880 的 AI0，AI1，AI2 和 AI3 接口分别送入数据采集卡 PCI-1713 的相应模拟通道 AI0，AI1，AI2 和 AI3，经 A/D 转换送入一体化工作站进行样本数据图形化显示与存盘。文中重点介绍信号适配电路和数据采集卡工作原理。

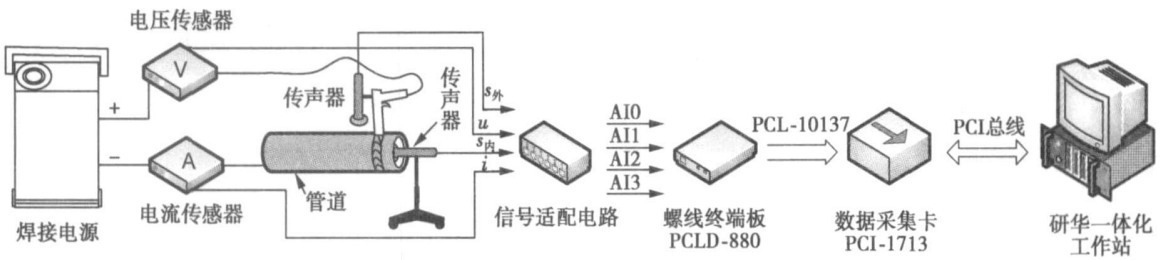

图 2 管道焊接电弧声发射采集系统原理图

Fig. 2 Schematic of collecting system for arc acoustic emission in pipe welding

2.2 信号适配电路

图 3 示出了整个信号适配电路的原理图，主要负责完成信号的放大、滤波、阻抗变换以及限幅等调理任务。焊接电流和电弧电压分别采用分流器和分压电阻获取，经运算放大器 LM358 放大，再经阻抗变换、限幅后由 PCLD-880 接口 AI0 和 AI1 进入 PCI-1713相应模拟通道 AI0 和 AI1。传声器拾取的电弧声信号比较微弱，首先通过 LM358 提高其分辨率。为了减少噪声影响，考虑到传声器的频率响应范围，采用 MAXIM 公司的集成芯片 MAX274 和 MAX263 设计了通带频率范围为 20～20 kHz 的带通滤波器。信号经滤波、阻抗变换以及限幅后由 PCLD-880 接口 AI2 和 AI3 进入 PCI-1713 相应模拟通道 AI2 和 AI3。

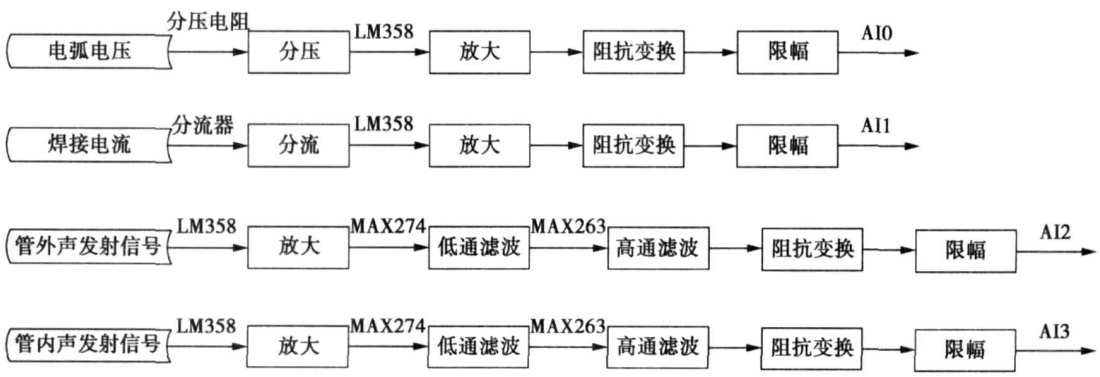

图 3 信号适配电路原理图

Fig. 3 Schematic of signal adaptor circuit

2.3 数据采集卡

系统使用基于 PCI 总线的 32 通道模拟量数据采集卡 PCI-1713，它采用 12 位高速 A/D 转换，采样率高达 100 kS/s，并在输入和 PCI 总线之间提供了

2 500 V的直流光隔离保护，用于保护 PC 及外围设备免受输入线上高压电的损害。PCI-1713 使用一个 PCI 控制器作为采集卡与 PCI 总线的接口，如图 4 所示。由于它支持 PnP（plug and play），其基地址及中断都由系统自动配置。

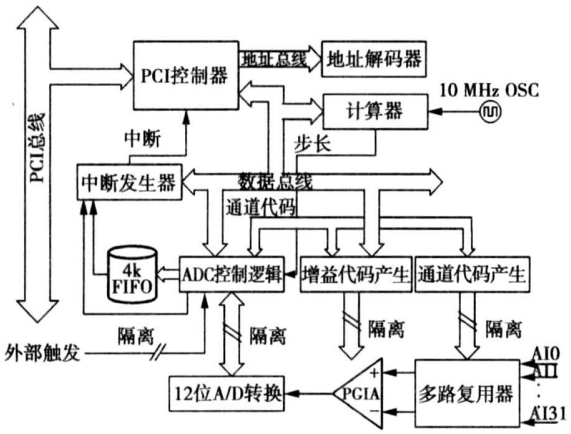

图 4　数据采集卡接线图

Fig. 4　Wiring diagram of data collecting card

3　采集系统软件设计

数据采集卡提供了 32 位的 LabVIEW 驱动程序，可调用 32 位 DLL 驱动程序的接口。在 LabVIEW 中，驱动函数以子 VIs（virtual instruments）的形式给出，通过对这些子 VIs 的调用，用户可以方便地访问底层寄存器，直接对板卡进行 I/O 操作。以上述硬件为平台，采用图形化虚拟仪器编程语言 LabVIEW，采用封装功能模块及调用硬件驱动的动态链接程序，设计了一个采用中断触发方式进行高速数据采集的焊接电弧声发射采集系统。电弧声信号长时间的高速实时数据采集，要用到内部缓冲区和用户缓冲区两块内存区域，采集的数据先写入内部缓冲区，再由内部缓冲区传送到用户缓冲区，然后就可以将数据以图形方式显示并存入文本文件。

内部缓冲区的使用采用循环方式。在这种方式下，内部缓冲区分为前后对等的两个半区使用，当内部缓冲区前半区满时，将此半区数据传送到用户缓冲区中，采集的数据继续向内部缓冲区的后半部分写入。当内部缓冲区全满时，将其后半部分数据传送到用户缓冲区中，同时新转换的数据会继续写入内部缓冲区的前半部分，如此反复，从而达到连续高速采集的功能，系统的软件流程图如图 5 所示。图中函数意义叙述如下，MultiChannelINTSetup：开始多通道中断触发方式的 A/D 转换，并将采集到的数据存储到内部缓存区，该操作将一直进行，直到调用 FAIStop 子 VI；WaitFastAIEvent：使程序进入等待状态，直到设定的事件发生（内部缓冲区半满或全满）或等待时间超出用户通过 Timeout 参数设定的值；AllocDSPBuf：为用户缓冲区分配参数 Count 指定大小的空间；FAITransfer：将数据从内部缓冲区传送到用户缓冲区。FAICheck：获得当前操作的状态，Half-Ready 显示内部缓冲区的状态，0 表示无任何半区满，1 表示前半区已满。

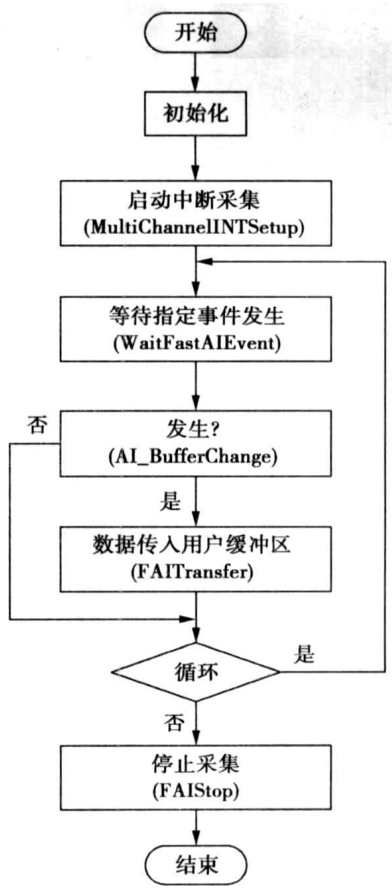

图 5　管道焊接电弧声发射信号采集软件流程图

Fig. 5　Software procedure of signal collecting for arc acoustic emission in pipe welding

4　采集系统测试试验

图 6 为管道 TIG 焊接试验装置，试验在 12Cr1MoV 钢钢管表面进行，管壁厚 35 mm，管径 400 mm，基值电流预设为 90 A，峰值电流预设为 220 A，占空比 2∶5，焊接速度330 mm/min，氩气流量 6.5 L/min。利用设计的焊接电弧声发射采集系统进行信号采集试验，采集系统可完成如下参数设置：触发源、A/D 转化次数、采样频率、采样通道数、各个通道增益、循环模式、循环等待时间、是否使用 FIFO

以及决定对指定事件源响应与否等，并且可将程序运行期间产生的错误来源显示于界面。采集系统人机界面如图 7 所示，试验表明该系统能实现对电弧电压、焊接电流和电弧声发射等模拟信号的高速实时同步采集，还能将采集结果以图形方式显示，解决了在文本编程语言下实时图形绘制难的问题。

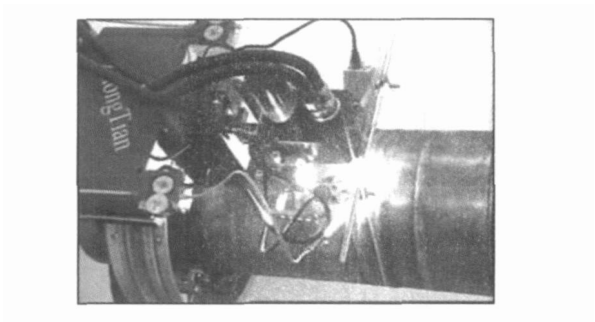

图 6 管道焊接试验装置

Fig. 6 Pipe welding experiment device

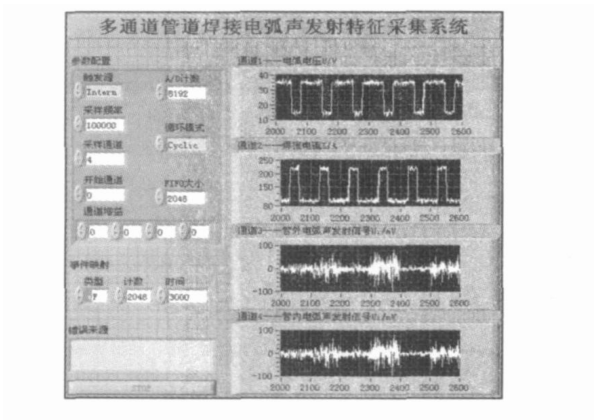

图 7 采集电弧模拟信号的实时人机界面

Fig. 7 Real-time HMI for collecting arc analog signals

5 结 论

(1) 针对电弧声发射信号与焊接熔透程度关系，研究主要集中在等离子弧小孔焊接和激光焊接方法，设计了管道焊接电弧声发射采集硬件系统，主要由传感器、信号适配电路、采集模块、一体化工作站以及焊接电源等部分组成，对管道 TIG 焊接电弧声发射机理进行了相关研究。

(2) 以管道焊接电弧声发射采集硬件系统为平台，借助图形化虚拟仪器编程语言 LabVIEW，采用封装功能模块及调用硬件驱动的动态链接程序，设计了一套采用中断触发方式进行高速数据采集的电弧声发射采集系统。

(3) 进行管道焊接电弧声发射采集系统测试试验。结果表明，该系统不仅能实现对电弧电压、焊接电流和电弧声发射等模拟信号的高速实时同步采集，还能将采集结果图形化显示，很好地解决了在文本编程语言下实时图形绘制难的问题，为进一步研究管道 TIG 焊接电弧声发射机理创造条件。

参考文献：

[1] 潘际銮，阎炳义，高力生，等. 爬行式全位置弧焊机器人[J]. 电焊机，2006，35(6)：1－5.

[2] 张 华，潘际銮，徐 健. 无轨导全位置爬行式弧焊机器人系统[J]. 机械工程学报，2006，42(7)：85－91.

[3] 刘京雷，陈彦宾，徐庆鸿. 激光焊接声信号与熔深的相关性[J]. 焊接学报，2006，27(1)：72－75.

[4] 武传松，赵朋成. 熔透熔池表面下塌变形的动态演变过程分析[J]. 金属学报，2006，42(8)：865－869.

[5] Ladislav G，Janez G. Feasibility study of acoustic for on-line monitory in short circuit gas metal arc welding[J]. International Journal of Machine Toll &Manufacture，2004，44(4)：551－561.

[6] Saini D，Floyd S. An investigation of gas metal arc welding sound signature for on-line quality control[J]. Welding Journal，1998，77(4)：172－179.

[7] Cudina M，Prezelj J. Evaluation of the sound signal based on the welding current in the gas-metal arc metal welding process[J]. Proceedings of the Institution of Mechanical Engineers，2003，217(5)：483－494.

[8] Ma Y Z，Qu M，Chen J. Characteristics analyzing and parametric modeling of the arc sound in CO_2 GMAW for on-line quality monitoring [J]. China Welding，2006，15(2)：13－18.

作者简介：刘立君，男，1968 年出生，博士，教授。主要从事焊接自动控制方面的科研和教学工作。发表论文 60 余篇。

Email：888liulijun@163.com

versity, Tianjin 300072, China). p17—19, 24

Abstract: Arc spraying and plasma cladding process was used to prepare the aluminum composite coating. The microstructure and phase structures of the clad alloy layer and the interface of alloy layer and steel matrix composites were analyzed. The results show that the tight alloy layer without pore and inclusion is obtained, and the coating and the steel are metallurgically compacted. The clad alloy layer consists of phase Fe_3Al, FeAl, α-Fe and Al_2O_3. Microhardness of the clad alloying layer will be 514 HV.

Key words: plasma cladding; Fe_3Al; intermetallic compound

Application of pre-scanning technology with laser to seam-curved tracking XIAO Zengwen, LIU Jifeng, CHEN Zhichao, GONG Xun (Department of Mechanical Engineering, Nanjing Institute of Technology, Nanjing 211167, China). p20—24

Abstract: The structured-light technology of traditional seam tracking makes front guiding error great if the curvature is varying. To solve the problem, a structured-light pre-scanning technology with double lines is produced. The seam is scanned before welding along the planned track of the robot. A laser line is added under the welding torch tip to indicate the front guiding error that will be recorded on time sequence and be eliminated when welding. A seam tracking system and its mathematical model are established. An image processing system is advanced, which the integrations of image processing technologies including median filtering, threshold transforming, thinness transforming and subsection beeline fitting locate the seam middle exactly. Tests show that the technology combined with the image processing system has the characteristics of strong anti-jamming, little error and fast processing speed, and it can meet the request of real time tracking.

Key words: seam tracking; structured-light; pre-scanning; image process; curved seam

Microstructure and shear strength of diffusion brazed Al_2O_3-TiC/Q235 joint WANG Juan[1], LI Yajiang[1], S. A. GERASIMOV[2] (1. Key Laboratory of Liquid Structure and Heredity of Materials, Shandong University, Jinan 250061, China; 2. Materials Science Department, Bauman Moscow State Technical University, Moscow 105005, Russia). p25—28

Abstract: An Al_2O_3-TiC/Q235 joint, Al_2O_3-TiC ceramic composite with steel Q235, was obtained by diffusion brazing in vacuum, using a combination of Ti and Cu as multi-interlayer. The interfacial strength was measured by shear testing and the result was explained by the fracture morphology. Microstructure of the Al_2O_3-TiC/Q235 joint was investigated by scanning electron microscope (SEM), energy-dispersion spectroscopy (EDS) and X-ray diffraction (XRD). The results indicate that the Al_2O_3-TiC/Q235 joint with a shear strength of 122 MPa can be obtained by controlling heating temperature at 1 110 ℃, multi-interlayer Ti/Cu/Ti is fused fully and diffused reaction to produce an obvious interfacial transition zone with a thickness of about 80 μm, and there are Ti_3AlC_2, Fe_2Ti, Cu and TiC in the transition zone.

Key words: Al_2O_3-TiC; diffusion brazing; shear strength; microstructure

Cross-section modeling of weld bead for rapid prototyping by MAG welding based on wavelet transform CAO Yong, ZHU Sheng, SUN Lei, SHEN Canduo, LIANG Yuanyuan, WANG Wanglong (National Defense Key Laboratory for Remanufacturing, Academy of Armored Forces Engineering, Beijing 100072, China). p29—32

Abstract: A new modeling method of weld bead profile by MAG welding process was proposed and the edge of the profile was extracted based on wavelet transform. The different interpolation methods, the cubic spline, the constrained cubic spline and the B-spline curve, were utilized respectively, the cross-section edge of weld bead was fitted by least square method, and then the mathematical model of the profile was achieved. The experimental results show that the method is effective to detect the cross-section outline of the profile, the constrained cubic interpolation is preferred choice to interpolate the data of the profile, and the cross-section profile mathematical model of weld bead is sine curve under our experiments.

Key words: rapid prototyping; wavelet transform; edge detection; modeling

Microstructure and wear resistance of plasma cladding Al_2O_3+TiO_2/Fe alloy composite coating LU Jinbin, LIANG Cun, PENG Zhuqin, ZHANG Zhaojun (College of Material and Chemical Engineering, Zhongyuan University of Technology, Zhengzhou 450007, China). p33—36

Abstract: Plasma cladding Ni-Cr-B-Si-Fe-based alloy coating and Fe-based alloy composite coating with Al_2O_3+TiO_2 were obtained on the Q235 substrate, and microstructure, microhardness and wear resistance of the two coatings were investigated contrastively. The results show that the interface solidification form of Fe-based alloy composite coating with Al_2O_3+TiO_2 have changed. They become small dendrite from primary lathy dendrite, and offer core for solidification. The microstructure is mainly based on γ-Fe with fine particles, and its microhardness can reach 600~655 HV0.2.

Key words: plasma cladding; microhardness; wear resistance; Al_2O_3+TiO_2

Data collecting system of pipe arc acoustic emission characteristics LIU Lijun[1,2], LAN Hu[1], DUAN Hongwei, WEN Jianli[1] (1. School of Material Science & Engineering, Harbin University of Science and Technology, Harbin 150080, China; 2. Ningbo Institute of Technology, Zhejiang University, Ningbo 315100, China). p37—40

Abstract: As the arc sound signal contains plenty of welding information which is an important source signal for welding quality control, arc acoustic emission signal (AAES) propagated in pipeline structure is low-noise, and AAES collecting system is designed for pipe TIG welding. The hardware system consists of sensor, signal adaptor circuit, data collecting card and industrial workstation. Based on virtual instrument programming software (LabVIEW), the high speed AAES collecting software system is designed by means of triggering interrupt, packaging function modules and calling dynamic

link programs of the hardware driver. The AAES experimental results show that the system not only correctly collects arc voltage, welding current and AAES at high speed synchronously, but also displays the real-time graph of the signals. The whole AAES collecting platform will lay the foundation for further studying on the arc acoustic emission mechanism in the pipe TIG welding.

Key words: pipe welding; arc acoustic emission; LabVIEW

Morphological analysis of interfacial reaction layers in Mo foil and Al foil jointing by diffusion bonding YANG Weihua[1], LI Jinglong[1], XIONG Jiangtao[1], ZHANG Fusheng[1], LÜ Xuechao[2] (1. Shaanxi Key Laboratory of Friction Welding Technologies, Northwestern Polytechnical University, Xi'an 710072, China; 2. China Academy of Engineering Physics, Mianyang 621000, China). p41—45

Abstract: Mo foil and Al foil were joined by diffusion bonding at 600 ℃ and 20 MPa for holding 50 min to 6 h to study the evolvements of the interface reactions at Mo-Al solid-solid interface. The results show that the new phases nucleate and form beneath the Mo substrate skin layer of 0.5—0.7 μm, then teare and lift off the Mo skin, turn to be island-like, and grow into Al substrate with Mo skin sandwiched. Initially, the reaction layers are not plane and like islands distributing along the interface, of which the growing rate is faster in longitudinal than in horizontal; with the islands further growing and joining together, three layers, Mo_3Al_8, $MoAl_5$ and $MoAl_{12}$, arise in sequence from Al-Mo interfacial reaction. When Al element is consumed, $MoAl_4$ phase grows up and forms a new layer between Mo_3Al_8 layer and $MoAl_5$ layer. At last, $MoAl_{12}$ and $MoAl_5$ are consumed and disappear with Mo_3Al_8 layer and $MoAl_4$ layer left on the interface.

Key words: Mo_3Al_8; $MoAl_5$; $MoAl_{12}$; interfacial reaction; diffusion bonding

Weld-softening zone width of 20MnSi controlled cooling bar LIANG Zhifang[1,2], WANG Yingna[1,2], LI Wushen[2], LIU Zhaohui[1], ZHANG Li[1] (1. North China Institute of Science & Technology, Beijing 101601, China; 2. Tianjin University, Tianjin 300072, China). p46—48

Abstract: When the 20MnSi controlled cooling bar is welded, there is a softened zone in the heat affect zone. The softened zone can diminish the load-bearing ability of the bar. By means of controlling the weld process variables and self-temper temperature, the weld-softening zone width can be controlled, and then the load-bearing ability can be improved. The relation model between the self-temper temperature and the welding parameters is gotten and analyzed by using the C.M. Adams formula. The results show that the weld-softening zone width decreases as the self-temper temperature increases, the weld-softening zone widens as the preheating temperature or the heat input increases, and the weld-softening zone of the smaller diameter of bar is wider than that of the bigger diameter of bar.

Key words: controlled cooling; self-temper temperature; heat affect zone; softened zone

Twin microstructure phase and formation mechanisms of aluminized coating ZHANG Wei[1], PANG Bijun[2], ZHANG Jinmin[3] (1. Department of Mechanical and Electrical Engineering, Luoyang Institute of Science and Technology, Luoyang 471023, China; 2. Mathematical Science College, Luoyang Normal University, Luoyang 471022, China; 3. Laboratory of Electron Microscopy, Luoyang Ship Material Research Institute, Luoyang 471039, China). p49—52

Abstract: The La-aluminized coating on 20-carbon-steel was prepared by hot dip aluminizing method. The microstructure of Al_4C_3 phase in the coating was investigated through transmission electron microscope (TEM) after diffusion treatment at 850 ℃ for 4 h. The results indicate that the Al_4C_3 phases are rod-shaped and approximately sphericized, and the twinned Al_4C_3 phases exist in the coating. By using conversion matrix of twin index and the conversion matrix acting on twin index, it is proved that the Al_4C_3 phases are 180° secondary rotation twin with (003) as twinning plane and [001] direction as twinning axis. The long axis direction of rod-shaped Al_4C_3 phases is parallel to (003) plane and perpendicular to [001] direction, and its long axis direction is [210] direction. This shows that there is 180° secondary rotation twin with (003) as twinning plane and [001] direction as twinning axis in hexagonal system. The formation mechanism of the twinned Al_4C_3 phases is also discussed in the paper.

Key words: hot dip aluminizing; diffusion treatment; twin; formation mechanism

Wear behavior of plasma sprayed nanostructured WC-17Co coatings at elevated temperature CHEN Hui[1], GOU Guoqing[1], LIU Yan[1], TU Mingjing[2] (1. Institute of Materials Science and Engineering, Southwest Jiaotong University, Chengdu 610031, China; 2. Institute of Materials Science and Engineering, Sichuan University, Chengdu 610041, China). p53—56, 60

Abstract: Wear is one of main material failure forms. Nanostructured WC-Co coating technology is expected to become a key technology to solve wear-resistance of critical components in large-scale equipments. Nanostructured and ultra-fine WC-17Co coatings were prepared by plasma spraying. The wear behavior at elevated temperature and failure mechanism were investigated. The results indicate that wear resistance at high temperature of the nanostructured WC-17Co coating is much better than that of the ultra-fine coating. The wear mechanism is different between the ultra-fine coating and the nanostructured coating, which low-ductility cracking and abrasive wear following with adhesive wear predominates in ultra-fine coating, and adhesive wear following with abrasive wear predominates in nanostructured coating.

Key words: nanostructured coatings; WC-17Co; elevated temperature wear

Twin-wire welding technology and corrosion resistance of weld seam for 7A52 aluminum alloy XIE Ruijun[1], CHEN Furong[1], ZHANG Chuanchen[1], GAO Yunxi[2] (1. College of Materials Science and Engineering, Inner Mongolia University of Technology, Hohhot